arXiv:hep-ph/0007012 v5 23 Nov 2001

CERN-TH/2000-337
DESY-00-179
UTHEP-00-0101

Precision Predictions for (Un)Stable W^+W^- Pair Production At and Beyond LEP2 Energies†

S. Jadach[a,b,c], **W. Płaczek**[d,c], **M. Skrzypek**[b,c], **B.F.L. Ward**[e,f,c] *and* **Z. Wąs**[b,c]

[a] *DESY-Zeuthen, Theory Division, D-15738 Zeuthen, Germany*
[b] *Institute of Nuclear Physics, ul. Kawiory 26a, 30-055 Cracow, Poland,*
[c] *CERN, Theory Division, CH-1211 Geneva 23, Switzerland,*
[d] *Institute of Computer Science, Jagellonian University, ul. Nawojki 11, 30-072 Cracow, Poland,*
[e] *Department of Physics and Astronomy, The University of Tennessee, Knoxville, Tennessee 37996-1200, USA,*
[f] *SLAC, Stanford University, Stanford, California 94309, USA.*

Abstract

We present precision calculations of the processes $e^+e^- \to 4$ fermions, in which the double resonant W^+W^- intermediate state occurs. Referring to this latter intermediate state as the signal process, we show that, by using the YFS Monte Carlo event generators YFSWW3-1.14 and KORALW 1.42 in an appropriate combination, we achieve a physical precision on the signal process, as isolated with LEP2 MC Workshop cuts, below 0.5%. We stress the full gauge invariance of our calculations and we compare our results with those of other authors where appropriate. In particular, sample Monte Carlo data are explicitly illustrated and compared with the results of the program RacoonWW of Denner *et al.* In this way, we show that the total (physical and technical) precision tag for the WW signal process cross section is 0.4% for 200 GeV, for example. Results are also given for 500 GeV with an eye toward future linear colliders.

Submitted to Phys. Lett. B

---

† Work partly supported by the Maria Skłodowska-Curie Joint Fund II PAA/DOE-97-316, the European Commission Fifth Framework contract HPRN-CT-2000-00149, and the US Department of Energy Contracts DE-FG05-91ER40627 and DE-AC03-76ER00515.

CERN-TH/2000-337
DESY-00-179
UTHEP-00-0101
November, 2000

The award of the 1999 Nobel Prize for physics to G. 't Hooft and M. Veltman, and the success of the predictions of their formulation [1] of the renormalized non-Abelian quantum loop corrections for the Standard Model [2] of the electroweak interactions in confrontation with data of LEP experiments, underscores the need to continue to test this theory at the quantum loop level in the gauge boson sector itself. This emphasizes the importance of the on-going precision studies of the processes $e^+e^- \to W^+W^- + n(\gamma) \to 4f + n(\gamma)$ at LEP2 energies [3–5], as well as the importance of the planned future higher energy studies of such processes in LC physics programs [6–9]. We need to stress that hadron colliders also have considerable reach into this physics and we hope to come back to their roles elsewhere [10].

In what follows, we present precision predictions for the event selections (ES) of the LEP2 MC Workshop [11], for the processes $e^+e^- \to W^+W^- + n(\gamma) \to 4f + n(\gamma)$, based on our new exact $\mathcal{O}(\alpha)_{prod}$ YFS-exponentiated LL $\mathcal{O}(\alpha^2)$ FSR leading-pole approximation (LPA) formulation, as it is realized in the MC program YFSWW3-1.14 [12, 13], in combination with all four-fermion processes MC event generator KoralW-1.42 [14, 15] so that the respective four-fermion background processes are taken into account in a gauge-invariant way. Indeed, gauge invariance is a crucial aspect of our work and we stress that we maintain it throughout our calculations. Here, FSR denotes final-state radiation and LL denotes leading-log as usual.

Recently, the authors in Refs. [16] have also presented MC program results for the processes $e^+e^- \to W^+W^- + n(\gamma) \to 4f + n(\gamma)$, $n = 0, 1$, in combination with the complete background processes that feature the exact LPA $\mathcal{O}(\alpha)$ correction. Thus, we will compare our results, where possible, with those in Refs. [16] in an effort to check the over-all precision of our work. As we argue below, the two sets of results should agree at a level below 0.5% on observables such as the total cross section.

More specifically, in YFSWW3-1.13 [13], the leading-pole approximation (LPA) is used to develop a fully gauge-invariant YFS-exponentiated calculation of the signal process $e^+e^- \to W^+W^- + n(\gamma) \to 4f + n(\gamma)$, which features the exact $\mathcal{O}(\alpha)$ electroweak correction to the production process and the $\mathcal{O}(\alpha^2)$ LL corrections to the final-state decay processes. The issue is how to combine this calculation with that of KoralW-1.42 in Ref. [14, 15] for the corresponding complete Born-level cross section with YFS-exponentiated initial-state $\mathcal{O}(\alpha^3)$ LL corrections. In this connection, we point out that the LPA enjoys some freedom in its actual realization, just as does the LL approximation in the precise definition of the big log L, without spoiling its gauge invariance. This can already be seen from the book of Eden *et al.* [17], wherein it is stressed that the analyticity of the S-matrix applies to the scalar form factors themselves in an invariant Feynman amplitude, without any reference to the respective external wave functions and kinematical (spinor) covariants. The classic example illustrated in Ref. [17] is that of pion–nucleon scattering, with the amplitude

$$\mathcal{M} = \bar{u}(p_2)[A(s,t) + B(s,t)(\not{q}_1 + \not{q}_2)]u(p_1), \tag{1}$$

where the p_i are the nucleon 4-momenta, the q_i are the pion 4-momenta, $u(p)$ is the usual Dirac wave function of the nucleon, and the invariant scalar functions $A(s,t)$ and $B(s,t)$ of the Mandelstam invariants $s = (p_1 + q_1)^2$, $t = (q_2 - q_1)^2$ realize the analytic properties

of the S-matrix themselves in the complex s and t planes. This means that, whenever we have spinning particles, we may focus on the analogs of A and B in eq. (1) in isolating the respective analytic properties of the corresponding S-matrix elements. We note that Stuart [18] has emphasized this point in connection with the production and decay of Z-pairs in e^+e^- annihilation and in connection with the production and decay of single W's in e^+e^- annihilation. What this means is that, in formulating the Laurent expansion of the S-matrix about its poles to isolate the dominant leading-pole term (the LPA is then realized by dropping all but this leading term), we may focus on only A and B, or we may insist that in evaluating the residues of the poles in the S-matrix the wave functions and kinematical covariants are also evaluated at the pole positions. When we focus only on the analogs of A and B in formulating the LPA, we shall refer to the result simply as the LPA$_a$; when we also evaluate the wave functions and kinematical covariants at the pole positions in isolating the poles in the analogs of A and B for the LPA, we shall refer to the respective result as the LPA$_b$. As Stuart stressed as well, both the LPA$_a$ and the LPA$_b$ are fully gauge-invariant.

For the process under discussion, a general representation is [18]

$$\mathcal{M} = \sum_j \ell_j A_j \left(\{q_k q_l\} \right) , \tag{2}$$

where $\{\ell_j\}$ are a complete set of kinematical covariants which carry the same transformation properties as does $\mathcal{M}$, and the Lorentz scalars $\{q_k q_l\}$ are a complete set of Lorentz scalar invariants for the external 4-momenta of $\mathcal{M}$. In the LPA$_a$, we make a Laurent expansion of the A_j and retain only their leading poles, without touching the $\{\ell_j\}$; in the LPA$_b$, we also evaluate the ℓ_j at the position of the respective leading poles. Evidently, in the latter case, we must make an analytic continuation of the phase-space point originally associated with the $\{\ell_j\}$ to a corresponding such point for the respective pole positions. See Ref. [12] for an illustration of such a continuation in the context of the YFS-exponentiated exact $\mathcal{O}(\alpha)$ calculation for the production process in $e^+e^- \to W^+W^- + n(\gamma) \to 4f + n(\gamma)$, and Refs. [5] for a similar illustration in the context of the $\mathcal{O}(\alpha)$ correction to $e^+e^- \to W^+W^- \to 4f$. Having isolated the appropriate realization of the LPA at the level of $\mathcal{M}$, it must still be decided whether to treat the phase space used to integrate the cross section exactly or approximately to match what was done for the $\{\ell_j\}$ in the case of the LPA$_b$. In all of our work, we stress that we always treat the exact phase space, both in the LPA$_a$ and in the LPA$_b$.

In the context of YFS exponentiation, we realize the LPA as follows, as was briefly described already in Ref. [12]. Taking the respective 4-fermion plus n-photon process kinematics to be as given by (here, $d\tau_{n+4}$ is the respective phase space differential with

the appropriate normalization):

$$
\begin{aligned}
&e^-(p_1)+e^+(p_2)\to f_1(r_1)+\bar f_2(r_2)+f_1'(r_1')+\bar f_2'(r_2')+\gamma(k_1),...,\gamma(k_n)\\
&\sigma_n=\frac{1}{flux}\int d\tau_{n+4}(p_1+p_2;r_1,r_2,r_1',r_2',k_1,...,k_n)\\
&\qquad\sum_{Ferm.\ Spin}\ \sum_{Phot.\ Spin}|\mathcal{M}_{4f}^{(n)}(p_1,p_2,r_1,r_2,r_1',r_2',k_1,...,k_n)|^2,
\end{aligned}
\tag{3}
$$

and that of the corresponding W^+W^- production and decay process to be as given by

$$
\begin{aligned}
&e^-(p_1)+e^+(p_2)\to W^-(q_1)+W^+(q_2),\\
&W^-(q_1)\to f_1(r_1)+\bar f_2(r_2),\quad W^+(q_2)\to f_1'(r_1')+\bar f_2'(r_2'),\\
&\sigma_n=\frac{1}{flux}\int d\tau_{n+4}(p_1+p_2;r_1,r_2,r_1',r_2',k_1,...,k_n)\\
&\qquad\sum_{Ferm.\ Spin}\ \sum_{Phot.\ Spin}|\mathcal{M}_{LPA}^{(n)}(p_1,p_2,r_1,r_2,r_1',r_2',k_1,...,k_n)|^2
\end{aligned}
\tag{4}
$$

in the context of YFS exponentiation [19,20], we proceed according to Refs. [12,19,20]

$$
\begin{aligned}
&\mathcal{M}_{4f}^{(n)}(p_1,p_2,r_1,r_2,r_1',r_2',k_1,...,k_n)\ \underset{=>}{^{LPA}}\ \mathcal{M}_{LPA}^{(n)}(p_1,p_2,r_1,r_2,r_1',r_2',k_1,...,k_n)\\
&=\sum_{Phot.\ Partitions}\mathcal{M}_{Prod}^{(a),\lambda_1\lambda_2}(p_1,p_2,q_1,q_2,k_1,...,k_a)\\
&\times\frac{1}{D(q_1)}\,\mathcal{M}_{Dec_1,\lambda_1}^{(b-a)}(q_1,r_1,r_2,k_{a+1},...,k_b)\ \times\frac{1}{D(q_2)}\,\mathcal{M}_{Dec_2,\lambda_2}^{(n-b)}(q_2,r_1',r_2',k_{b+1},...,k_n),\\
&D(q_i)=q_i^2-M^2,\quad M^2=(M_W^2-i\Gamma_W M_W)(1-\Gamma_W^2/M_W^2+\mathcal{O}(\alpha^3)),\\
&q_1=r_1+r_2+k_{a+1}+...+k_b;\ \ q_2=r_1'+r_2'+k_{b+1}+...+k_n,
\end{aligned}
\tag{5}
$$

so that M^2 is the pole in the complex q^2 plane when q is the respective W 4-momentum, and M_W and Γ_W are the *on-shell* scheme mass and width, respectively. The residues in (5) are all defined at $q_i^2=M^2$ with a prescription according to whether we have LPA_a or LPA_b, so that (5) is our YFS generalization of the formula in eq. (12) in the first paper in Ref. [5]:

$$
\mathcal{M}^{(n)}=\sum_{\lambda_1,\lambda_2}\Pi_{\lambda_1,\lambda_2}(M_1,M_2)\frac{\Delta_{\lambda_1}^+(M_1)}{D_1}\,\frac{\Delta_{\lambda_2}^-(M_2)}{D_2},\ n=0,1,
\tag{6}
$$

where $D_i=D(q_i)$ and $M_i^2=M^2$. We stress that, unlike what is true of the formula in eq. (12) in the first paper in Ref. [5] and in eq. (6) here, in eq. (5) n is arbitrary. The sum over "photon partitions" is over all 10^n possible attachments of n photons to the six external fermion lines and the two $W^\pm$ lines (one for the W production and one for the W decay, respectively). We make the further approximation that $M_i^2=M_W^2$ in the residues in (5), always maintaining gauge invariance, as explained. Equations (3) and (4)

in Ref. [21] then give us, in the presence of renormalization-group-improved perturbation theory, for the representation

$$\mathcal{M}^{(n)}_{LPA}(p_1,p_2,r_1,r_2,r'_1,r'_2,k_1,...,k_n)=\sum_{j=0}^{\infty}\mathcal{M}^{(n)}_{j}(p_1,p_2,r_1,r_2,r'_1,r'_2,k_1,...,k_n), \tag{7}$$

where $\mathcal{M}^{(n)}_{j}$ is the j-th virtual photon loop contribution to the residues in $\mathcal{M}^{(n)}_{LPA}$, the identifications

$$\mathcal{M}^{(n)}_{j}(p_1,p_2,r_1,r_2,r'_1,r'_2,k_1,...,k_n)=\sum_{r=0}^{j}\mathfrak{m}^{(n)}_{j-r}\frac{(\alpha B')^r}{r!}, \tag{8}$$

where B' is now, for the LPA$_b$ case to be definite, the **on-shell** virtual YFS infrared function, which reduces to that given in eqs. (8) and (9) in Ref. [20] when we restrict our attention to the production process, and α is indeed $\alpha(0)$ when it multiplies B' here. Let us keep this limit of B' in mind, as we focus on the gauge invariance of YFSWW3-1.11 in Ref. [12], which treats the radiation in the production process, and on that of YFSWW3-1.13 and YFSWW3-1.14, in which the radiation from the decay processes is also treated. In the LPA$_a$ case, the corresponding B' function is **off-shell**. Let us discuss first the LPA$_b$ case and comment later on how the corresponding results for the LPA$_a$ case are obtained.

Here, since the $SU(2)_L\times U(1)$ Ward–Takahashi identities require (see eq. (47) in Ref. [22])

$$k^\mu M^\gamma_\mu=0,\quad k^\mu M^Z_\mu=i\sqrt{\mu_Z}M^\chi,\quad k^\mu M^{W^\pm}_\mu=\pm\sqrt{\mu_W}M^{\phi^\pm}, \tag{9}$$

for μ_V denoting the squared V boson mass (so that, for $V=W$, $\mu_W=M^2$), we find that B' is $SU(2)_L\times U(1)$-invariant from the equations in (9) and our result eq. (8) in Ref. [20]. From eq. (8) it then follows that the infrared residuals $\mathfrak{m}^{(n)}_{j-r}$ are also $SU(2)_L\times U(1)$-invariant. Here, χ and $\phi^\pm$ are the usual unphysical Higgs fields in our general renormalizable gauges and we use the notation of Ref. [22], so that M^Z_μ is their respective amplitude for the emission of a Z of Lorentz index μ and 4-momentum k, and M^χ is their corresponding amplitude for the emission of a χ with the same 4-momentum, etc.

Introducing eq. (8) into (7) gives

$$\mathcal{M}^{(n)}_{LPA_b}(p_1,p_2,r_1,r_2,r'_1,r'_2,k_1,...,k_n)=e^{\alpha B'}\sum_{j=0}^{\infty}\mathfrak{m}^{(n)}_{j}(p_1,p_2,r_1,r_2,r'_1,r'_2,k_1,...,k_n). \tag{10}$$

Equation (2.13) in Ref. [19] and eq. (7) in Ref. [21] then give our n-photon differential cross section, for $P=p_1+p_2$, $\vec{P}=0$, as

$$d\sigma^n_{LPA_b}=e^{2\Re\alpha B'}\frac{1}{n!}\int\prod_{j=1}^{n}\frac{d^3k}{k_j^0}\delta^{(4)}\left(P-R-\sum_j k_j\right)\left|\sum_{n'=0}^{\infty}\mathfrak{m}^{(n)}_{n'}\right|^2\frac{d^3r_1}{r_1^0}\frac{d^3r_2}{r_2^0}\frac{d^3r'_1}{r'^0_1}\frac{d^3r'_2}{r'^0_2}, \tag{11}$$

where we note that, when we only focus on the production process in eq. (11), R is the produced WW intermediate state; $R = r_1 + r_2 + r_1' + r_2'$. Using the second theorem of the YFS program (eq. (2.15) in [19]), we get

$$\begin{aligned}\left|\sum_{n'=0}^{\infty} \mathfrak{m}_{n'}^{(n)}\right|^2 &= \tilde{S}(k_1)\cdots\tilde{S}(k_n)\bar{\beta}_0 + \sum_{i=1}^{n}\tilde{S}(k_1)\cdots\tilde{S}(k_{i-1})\tilde{S}(k_{i+1})\cdots\tilde{S}(k_n)\bar{\beta}_1(k_i) \\ &+ \cdots + \sum_{i=1}^{n}\tilde{S}(k_i)\bar{\beta}_{n-1}(k_1,\cdots,k_{i-1},k_{i+1},\cdots,k_n) + \bar{\beta}_n(k_1,\cdots,k_n),\end{aligned} \tag{12}$$

where the real emission function $\tilde{S}(k)$ is given by $\tilde{S}_{Prod}(k)$, the real emission infrared function in eq. (8) in Ref. [20] for **on-shell** $W's$, when we only focus on the emission from the production process as we did in Refs. [12, 13]. Since, in general,

$$\tilde{S}(k) = \tilde{S}_{Prod} + \tilde{S}_{Dec_1} + \tilde{S}_{Dec_2} + \tilde{S}_{Int}, \tag{13}$$

with

$$\begin{aligned}\tilde{S}_{Prod}(k) = -\frac{\alpha}{4\pi^2}\Bigg[&\left(\frac{p_1}{kp_1} - \frac{p_2}{kp_2}\right)^2 + \left(\frac{\mathcal{A}q_1}{k\mathcal{A}q_1} - \frac{\mathcal{A}q_2}{k\mathcal{A}q_2}\right)^2 \\ &+ \left(\frac{p_1}{kp_1} - \frac{\mathcal{A}q_1}{k\mathcal{A}q_1}\right)^2 + \left(\frac{p_2}{kp_2} - \frac{\mathcal{A}q_2}{k\mathcal{A}q_2}\right)^2 \\ &- \left(\frac{p_1}{kp_1} - \frac{\mathcal{A}q_2}{k\mathcal{A}q_2}\right)^2 - \left(\frac{p_2}{kp_2} - \frac{\mathcal{A}q_1}{k\mathcal{A}q_1}\right)^2\Bigg]\Bigg|_{(\mathcal{A}q_i)^2=M_W^2},\end{aligned} \tag{14}$$

$$\begin{aligned}\tilde{S}_{Dec_1}(k) = -\frac{\alpha}{4\pi^2}\Bigg[&Q_1Q_2\left(\frac{r_1}{kr_1} - \frac{r_2}{kr_2}\right)^2 - Q_1Q_W\left(\frac{r_1}{kr_1} - \frac{\mathcal{A}q_1}{k\mathcal{A}q_1}\right)^2 \\ &+ Q_2Q_W\left(\frac{r_2}{kr_2} - \frac{\mathcal{A}q_2}{k\mathcal{A}q_2}\right)^2\Bigg]\Bigg|_{(\mathcal{A}q_1)^2=M_W^2},\end{aligned} \tag{15}$$

$$\begin{aligned}\tilde{S}_{Dec_2}(k) = -\frac{\alpha}{4\pi^2}\Bigg[&Q_1'Q_2'\left(\frac{r_1'}{kr_1'} - \frac{r_2'}{kr_2'}\right)^2 + Q_1'Q_W\left(\frac{r_1'}{kr_1'} - \frac{\mathcal{A}q_2}{k\mathcal{A}q_2}\right)^2 \\ &- Q_2'Q_W\left(\frac{r_2'}{kr_2'} - \frac{\mathcal{A}q_2}{k\mathcal{A}q_2}\right)^2\Bigg]\Bigg|_{(\mathcal{A}q_2)^2=M_W^2},\end{aligned} \tag{16}$$

$$\begin{aligned}\tilde{S}_{Int}(k) = -\frac{\alpha}{4\pi^2}\Big(&\frac{p_1}{kp_1} - \frac{p_2}{kp_2} + Q_1\frac{r_1}{kr_1} - Q_2\frac{r_2}{kr_2} \\ &+ Q_1'\frac{r_1'}{kr_1'} - Q_2'\frac{r_2'}{kr_2'}\Big)^2 - \tilde{S}_{Prod} - \tilde{S}_{Dec_1} - \tilde{S}_{Dec_2}\end{aligned} \tag{17}$$

is really composed of the scalar product of emission currents $\{j_b^\mu(k)\}$ with $k_\mu j_b^\mu(k) = 0$, eq. (13) is also $SU(2)_L \times U(1)$-invariant. Here

$$\mathcal{A}q_i \equiv \text{analytical continuation of } \; q_i \text{ to the point } q_i^2 = M_W^2. \tag{18}$$

This analytical continuation, already described in Ref. [12], does not spoil the gauge invariance, as we see from Eqs. (13,18). It follows that the hard-photon residuals $\{\bar{\beta}_n\}$ are also $SU(2)_L \times U(1)$-invariant.

Substitutung (12) into (11) we finally get the $SU(2)_L \times U(1)$-invariant expression, which is the fundamental formula of our calculation,

$$\begin{aligned} d\sigma_{LPA_b} = {} & e^{2\Re\alpha B' + 2\alpha\tilde{B}} \frac{1}{(4\pi)^4} \int d^4y e^{iy(p_1+p_2-q_1-q_2)+D} \\ & \times \left[\bar{\beta}_0 + \sum_{n=1}^{\infty} \frac{d^3k_j}{k_j^0} e^{-iyk_j} \bar{\beta}_n(k_1,...,k_n)\right] \frac{d^3r_1}{\bar{r}_1^0} \frac{d^3r_2}{r_2^0} \frac{d^3r_1'}{\bar{r'}_1^0} \frac{d^3r_2'}{\bar{r'}_2^0}, \end{aligned} \tag{19}$$

where we have defined

$$D = \int \frac{d^3k}{k_0} \tilde{S} \left[e^{-iy\cdot k} - \theta(K_{max} - |\vec{k}|)\right], \quad 2\alpha\tilde{B} = \int \frac{d^3k}{k_0} \theta(K_{max} - |\vec{k}|)\tilde{S}(k). \tag{20}$$

This shows that the parameter $K_{max} \ll \sqrt{s}$ is a dummy parameter on which $d\sigma$ does not depend. In (19), when the complete value of $\tilde{S}(k)$ is used, then all $W^\pm$ radiative effects are contained in the respective $\bar{\beta}_n$ residuals, in accordance with the YFS theory in Ref. [19], as the non-zero widths of the W's prevent any IR singularities when a W radiates a photon in (4). In our work in YFSWW3, as we indicate below, we make the approximation of dropping all interference effects between the production and decay stages and between the two decay stages of (4). This means that we drop the $\tilde{S}_{Int}(k)$ in $\tilde{S}(k)$ in (13) and in (19), so that the YFS theory then determines the corresponding forms of the YFS functions $\bar{\beta}_n$, B' and D as also having the respective interferences dropped. This approximation, which resums a certain class of large W radiative effects, corresponds to the YFS exponentiation of the W production and decay radiation in the LPA, neglecting of all interferences between the production and decay stages and between the two decay processes.

We will now comment further on our use of (19). Since the residuals on the RHS (right-hand side) of (5) are on-shell amplitudes in the $SU(2)_L \times U(1)$ theory, for both the production and the decay process, it follows that they satisfy the renormalization group equations [23,24] for the $SU(2)_L \times U(1)$ theory, as explained in Ref. [21]:

$$\left(\mu\frac{\partial}{\partial\mu} + \beta_j(\{g_{iR}\})\frac{\partial}{\partial g_{jR}} - \gamma_{\Theta_j}(\{g_{iR}\})m_{jR}\frac{\partial}{\partial m_{jR}} - \gamma_\Gamma(\{g_{iR}\})\right)\Gamma = 0 \tag{21}$$

for $\Gamma = \mathcal{M}_{Prod}^{(n)\lambda_1,\lambda_2}, \mathcal{M}_{Dec,\lambda_i}^{(n')}$, where μ is the arbitrary renormalization point, $\{g_{iR}\}$ are the respective renormalized $SU(2)_L \times U(1)$ couplings, and $\{m_{iR}\}$ are the corresponding

renormalized mass parameters, etc., as defined in Ref. [24]. It follows that any two schemes for computing $\mathcal{M}_{Prod}^{(n)\lambda_1,\lambda_2}, \mathcal{M}_{Dec,\lambda_i}^{(n')}$ are related by a finite renormalization-group transformation. Thus, the complex pole scheme (CPS) and the fermion loop scheme (FLS) [25] values of $\mathcal{M}_{Prod}^{(n)\lambda_1,\lambda_2}, \mathcal{M}_{Dec_i,\lambda_i}^{(n')}$ are related by such a finite renormalization-group transformation. Specifically, if we denote CPS and FLS values of any quantity A by A(CPS) and A(FLS), respectively, then we have the identity

$$Z_{\Gamma(CPS)}^{-1}\Gamma(\mathrm{CPS}) = \Gamma_{un} = Z_{\Gamma(\mathrm{FLS})}^{-1}\Gamma(\mathrm{FLS}), \tag{22}$$

where Γ_{un} is the respective unrenormalized value of Γ and the $Z_{\Gamma(\mathrm{R})}$, R = CPS, FLS are the respective field renormalization constants. It therefore follows that we have the finite renormlization group transformation

$$\Gamma(\mathrm{CPS}) = Z_{\Gamma(\mathrm{CPS})}Z_{\Gamma(\mathrm{FLS})}^{-1}\Gamma(\mathrm{FLS}) \tag{23}$$

connecting the FLS and CPS schemes. Of course, as the usual implementation of the FLS scheme omits a gauge invariant set of contributions to the heavy vector boson widths, for example, in checking the the result in (23) we must omit the corresponding contributions on both sides of the equation for consistency, as is usualy the case when we compare renormalzation group improved quantities. Indeed, as we take the normalization points for the two schemes to be the complex pole position $M^2 = \mu_W$, and as we evaluate $\mathcal{M}_{Prod}^{(n)\lambda_1,\lambda_2}, \mathcal{M}_{Dec_i,\lambda_i}^{(n')}$ at this normalization point, the only difference in using the FLS instead of the CPS will be the approximate treatment in the FLS of the actual values of $\mathcal{M}_{Prod}^{(n)\lambda_1,\lambda_2}, \mathcal{M}_{Dec_i,\lambda_i}^{(n')}$, and μ_W for the pole position, as already shown in eq. (8) of the first paper in Ref. [5]: thus, for example, if we keep only fermion loops in $\mathcal{O}(\alpha)$, only the lowest-order width appears in eq. (6) of the first paper in Ref. [5]; thus if one would express the resulting $\mu_W = M^2$ in terms of the respective on-shell mass and width, only the lowest-order part of Γ_W would be given properly. Similarly, as both schemes normalize at μ_W, the difference in the residues $\mathcal{M}_{Prod}^{(n)\lambda_1,\lambda_2}, \mathcal{M}_{Dec_i,\lambda_i}^{(n')}$ is that in the FLS only the fermion-loop contributions are retained, whereas the CPS keeps all loops. Evidently, we may extend our $\mathcal{O}(\alpha)$ calculation in the FLS by using the complete value of μ_W and including all the one-loop corrections and attendant $\mathcal{O}(\alpha)$ real corrections from Ref. [26], as we did in Ref. [12]. We conclude that, after adding in the entire $\mathcal{O}(\alpha)$ correction from Ref. [26], our LPA exact $\mathcal{O}(\alpha)_{prod}$ YFS-exponentiated calculation arrives at the same amplitudes, independent of whether we started with the FLS or the CPS.

All of the above results extend directly to the calculation when we use LPA$_a$ amplitudes, as these are also gauge-invariant by the gauge-invariance of our leading poles in the S-matrix. Thus, the only change we must make is that the respective residues must be calculated in the LPA$_a$ rather than in the LPA$_b$; for example, in eqs. (14-17), q_i would be used instead of $\mathcal{A}q_i$, etc. We have done this, as we further illustrate in the following.

Let us now comment on the issue of the pure FSR YFS exponentiation for the decay processes treated in the LPA. We proceed in analogy to what is done in Ref. [27] for the MC YFS3 for the respective FSR. Specifically, for both decay residue amplitudes $\mathcal{M}_{Dec_i,\lambda_i}^{(n')}$, we may have contributions to the respective hard-photon residuals $\bar{\beta}_n$ due to

emission for the final-state decay processes; in these we follow the procedure, described in Refs. [27,28] and already illustrated in Ref. [29], for including these contributions, using the same YFS methods as we used above for radiative effects to the initial, intermediate and final states. Here, we shall neglect all interference effects between the production and decay processes as we explained above; this is analogous neglecting all interference effects between the initial and final states in the $\bar{\beta}_n$ in Refs. [27, 29]. We note that it is possible to retain these interference effects, as we have illustrated in the exact $\mathcal{O}(\alpha)$ YFS-exponentiated BHWIDE MC in Ref. [30] for wide-angle Bhabha scattering and, more recently, using the new CEEX exponentiation theory in Ref. [31], to all orders in α in the new KK MC [28, 31] for the 2 fermion processes from the τ threshold to 1 TeV. In this way we see that the use of eq. (19) to include exponentiation of the FSR is fully realizable by Monte Carlo methods we already tested. We stress that, for the same reasons as we gave for the exponentiation of the complete process, these FSR contributions to the $\bar{\beta}_n$ are fully gauge-invariant.

In the current version of YFSWW3, version 1.14, we also drop the $\tilde{S}_{Dec_i}$ terms in $\tilde{S}$ in eq. (13) and the corresponding terms in the functions $\bar{\beta}_n$, B' and D, and include FSR using the program PHOTOS [32], which gives us a LL $\mathcal{O}(\alpha^2)$ realization of the FSR in which finite p_T effects are represented as they are in the $\mathcal{O}(\alpha)$ soft-photon limit. This LL implementation of FSR is fully gauge-invariant. The ratio of BRs is then used to obtain the $\mathcal{O}(\alpha)$ correction in the normalization associated with the $\mathcal{O}(\alpha)$ correction to the decay processes themselves. Evidently, these ratios of BRs are also gauge-invariant. As we illustrate below, for the corresponding non-factorizable corrections we use an efficient approximation in terms of the so-called screened Coulomb ansatz [33], which has been shown to be in good agreement with the exact calculations for singly inclusive distributions [33]. This ansatz is gauge-invariant.

We also point out that the current version 1.14 differs from version 1.13 in Ref. [13] in that it uses a different renormalization scheme. Specifically, the scheme used in version 1.13 is the so-called G_μ of Ref. [26], in which the weak-scale coupling [26] α_{G_F} is used for all terms in the virtual correction, except those that are infrared-singular, which are given the coupling $\alpha \equiv \alpha(0)$. In the renormalization-group-improved YFS theory, as formulated in Ref. [21], all the terms in the amplitude that involve corrections, in which the emitted photon of 4-momentum k has $k^2 \to 0$, should have the coupling strength corresponding to $\alpha(0)$ – not just those that are IR singular. We therefore have introduced into YFSWW3 this requirement of the renormalization-group-improved YFS theory to arrive at version 1.14. We refer to this scheme as our scheme (A). According to the renormalization-group-improved YFS theory, it gives a better representation of the higher orders effects than does the G_μ scheme of Ref. [26]. We stress that this scheme (A) is also gauge-invariant. The main effect of this change in renormalization scheme between versions 1.13 and 1.14 is to change the normalization of version 1.14 by $\sim -0.3\%$ to -0.4% with respect to that of version 1.13 [11].

The generic size of the resulting shift in the YFSWW3 prediction, which we just quoted, can be understood by isolating the well-known soft plus virtual LL ISR correction

to the process at hand, that has in $\mathcal{O}(\alpha)$ the expression [26]

$$\delta^{v+s}_{ISR,LL} = \beta \ln k_0 + \frac{\alpha}{\pi}\left(\frac{3}{2}L + \frac{\pi^2}{3} - 2\right), \tag{24}$$

where $\beta \equiv \frac{2\alpha}{\pi}(L-1)$, $L = \ln(s/m_e^2)$, and k_0 is a dummy soft cut-off that cancels out of the cross section as usual. In the G_μ scheme of Refs. [26], which is used in YFSWW3-1.13, only the part $\beta \ln k_0 + (\alpha/\pi)(\pi^2/3)$ of $\delta^{v+s}_{ISR,LL}$ has the coupling $\alpha(0)$ and the remaining part of $\delta^{v+s}_{ISR,LL}$ has the coupling $\alpha_{G_\mu} \cong \alpha(0)/(1-0.0371)$. The renormalization-group-improved YFS theory implies, however, that $\alpha(0)$ should be used for all the terms in $\delta^{v+s}_{ISR,LL}$. This is done in YFSWW3-1.14 and results in the normalization shift $\left((\alpha(0) - \alpha_{G_\mu})/\pi\right)(1.5L-2)$, whichis $\sim -0.33\%$ at 200 GeV. This explains most of the change in the normalization of YFSWW3-1.14 with respect to YFSWW3-1.13. Moreover, it does not contradict the expected total precision tag of either version of YFSWW3 at their respective stages of testing. We stress that, according to the renormalization-group equation, version 1.14 is an improvement over version 1.13 in that it better represents the true effect of the respective higher-order corrections.

For the purposes of cross checking with ourselves and with Ref. [16], we also created a second scheme, scheme (B), for the realization of the renormalization in YFSWW3-1.14. In this scheme, we put the entire $\mathcal{O}(\alpha)$ correction from Refs. [26] at the coupling strength $\alpha = \alpha(0)$. Since the pure NL hard $\mathcal{O}(\alpha)$ correction is only ~ -0.006 at 200 GeV, scheme (B) differs in the normalization from scheme (A) by $\sim (\alpha(0)/\alpha_{G_\mu} - 1)(-0.006) \cong 0.0002$, which is well below the 0.5% precision tag regime of interest for LEP2. Thus, scheme (B), which is used in Ref. [16], is a perfectly acceptable scheme for LEP2 applications. It gives us a useful reference point from which to interpret our comparison with the results of RacoonWW from Ref. [16], which we discuss below.

Having presented our gauge-invariant calculation as it is realized in the MC YFSWW3-1.14, we will now turn to illustrating it in the context of LEP2 applications. Specifically, we always have in mind that one will combine the cross section from YFSWW3 with that from KoralW-1.42 [14,15] MC, which is capable to calculate the non-resonant background contribution in a gauge-invariant way. We can do this in two ways, which we will now briefly describe and refer the reader to Refs. [34] for the more detailed discussion. In the first way, we start with LPA$_a$ and we denote the corresponding cross section from YFSWW3-1.14 as $\sigma(Y_a)$. It is corrected for the missing background contribution by adding to it a correction $\Delta\sigma(K)$ from KoralW-1.42 to form

$$\sigma_{Y/K} = \sigma(Y_a) + \Delta\sigma(K), \tag{25}$$

where $\Delta\sigma(K)$ is defined by

$$\Delta\sigma(K) = \sigma(K_1) - \sigma(K_3). \tag{26}$$

Here, the cross section $\sigma(K_1)$ is the complete 4-fermion result from KoralW-1.42 with all background diagrams and with the YFS-exponentiated $\mathcal{O}(\alpha^3)$ LL ISR and the cross

section $\sigma(K_3)$ is the restricted CC03 Born-level result from KoralW-1.42 – again with the YFS-exponentiated $\mathcal{O}(\alpha^3)$ LL ISR. The result in eq. (25) is then accurate to $\mathcal{O}(\frac{\alpha}{\pi}\frac{\Gamma_W}{M_W})$. Alternatively, one may start with the cross section for LPA$_{a,b}$ in YFSWW3-1.14, which we refer to as $\sigma(Y_a)$ and $\sigma(Y_b)$ correspondingly, and isolate the respective YFS-exponentiated $\mathcal{O}(\alpha)$ correction, $\Delta\sigma(Y)$, which is missing from the cross section $\sigma(K_1)$ as

$$\Delta\sigma(Y_j) = \sigma(Y_j) - \sigma(Y_4), \tag{27}$$

where $\sigma(Y_4)$ is the corresponding cross section from YFSWW3-1.14, with the non-leading (NL) non-ISR $\mathcal{O}(\alpha)$ corrections to $\bar{\beta}_n$, $n = 0, 1$, switched off. Then the cross section

$$\sigma_{K/Y} = \sigma(K_1) + \Delta\sigma(Y_j) \tag{28}$$

has the accuracy of $\mathcal{O}(\frac{\alpha}{\pi}\frac{\Gamma_W}{M_W})$. We have checked that the results $\sigma_{Y/K}$ and $\sigma_{K/Y}$ are numerically equivalent at the 0.1% level of interest to us here. In the following we only show results from the former. For completeness, we also note that we sometimes identify $\sigma(Y_1) = \sigma(Y_a)$, $\sigma(Y_2) = \sigma(Y_b)$, $\sigma(Y_3) = \sigma(K_3)$, and $\sigma(K_2)$ is to be identified as the cross section from KoralW-1.42 with the restricted on-pole CC03 Born-level matrix element with YFS-exponentiated $\mathcal{O}(\alpha^3)$ LL ISR. This latter cross section is a future option of KoralW [10]. It would allow further combinations of YFSWW3 and KoralW with the desired $\mathcal{O}(\frac{\alpha}{\pi}\frac{\Gamma_W}{M_W})$ accuracy. Such combinations would be of use in cross checks of our work.

We now illustrate our precision predictions using $\sigma_{Y/K}$. We have checked that the correction $\Delta\sigma(K)$ is small, $\lesssim 0.1\%$ for CMS energies $\sim 200\,\mathrm{GeV}$. This is summarized in Tables 1 and 2, in which we compare the size of the correction $\Delta\sigma(K)$, labeled δ_{4f}, with the size of the respective NL non-ISR $\mathcal{O}(\alpha)$ correction for the 4-lepton, 2-lepton–2-quark, and 4-quark final states, with and without the cuts of Ref. [11] at 200 GeV.

Thus, in what follows, we shall ignore $\Delta\sigma(K)$, as our ultimate precision tag objective, $< 0.5\%$, does not require that we keep it. It will be analyzed in more detail elsewhere [10]. Further, for the cross section $\sigma(Y_a)$ we have already presented, for version 1.13, in Figs. 1-8 of Ref. [13], for the $c\bar{s}\ell\bar{\nu}_\ell$, $\ell = e^-, \mu^-$ final states, the $W^{+,-}$ angular distributions in the e^+e^- CMS system, the $W^{+,-}$ mass distributions, the distributions of the final-state lepton energies in the LAB frame (e^+e^- CMS frame), and the final-state lepton angular distributions in the W^- rest frame their corrections (relative to the Born-level). The main effect on these differential distributions of the improved normalization of version 1.14 is to shift the normalization, as we discussed above. Thus, we do not repeat their presentation here. We refer the reader to the results in Ref. [13] for an investigation into the size of the EW=NL and FSR effects in the cases listed above insofar as YFSWW3-1.14 is concerned with the understanding that the shapes of the distributions apply directly to version 1.14, but that the normalization of the EW correction should be reduced by -0.3% to -0.4%. In general, we found in Ref. [13] that, depending on the experimental cuts and acceptances, both the FSR and the EW corrections were important in precision studies of these distributions; this conclusion still holds for version 1.14, of course. For example, in the lepton decay angle distribution, for the BARE acceptance (the final charged lepton is

not combined with any photons), where both the FSR and the EW correction modulate the distribution, whereas for the CALO acceptance of Ref. [13] (all photons within 5° of the final-state charged lepton are combined with it) the FSR effect is almost nil whereas the EW correction effect remains at the level of $\sim 2.0\%$. Here, we focus on the total CMS photon energy distribution (Fig. 1a), and the CMS photon angular distribution (Fig. 1b). We show these results both for the BARE and CALO acceptances, as defined in the 4 fermion Section of the Proceedings of the LEP2 MC Workshop [11].

In Fig. 1a, we see that the total photon energy distributions are different for the BARE and CALO cases but that the NL non-ISR correction does not affect them strongly. In Fig. 1b, we see that, for both the BARE and CALO cases, the NL correction does affect the photon angular distribution away from the beam directions, as we expect. Note that this is the NL correction implied by the YFS exponentiation of our exact $\mathcal{O}(\alpha)_{prod}$ correction. Finally, in Fig. 2, we show the effect, in the W mass and angular distributions, of using the screened Coulomb correction from Ref. [33], as against the usual Coulomb correction from Ref. [35]. The effect we see is a 5 MeV shift in the peak position, associated with the difference between the screened and usual Coulomb corrections; we see almost no effect, as expected, associated with this difference on the e^+e^- CMS W angular distribution. Since we calculate the finite p_T $n(\gamma)$ corrections to these distributions, these results are new. Indeed, in Ref. [11] it is shown that the results from RacoonWW and YFSWW3 (Best) for the distribution in Fig. 1a differ by $\sim 20\%$ and, as we have the dominant $\mathcal{O}(\alpha^2)$ LL corrections to this distribution whereas in Fig. 20 in Ref. [11] the RacoonWW result only has the exact $\mathcal{O}(\alpha)$ Born result for the hard photon observable, we expect that most of this discrepancy would be removed if the dominant $\mathcal{O}(\alpha^2)$ LL corrections were included in the RacoonWW results. This has recently been confirmed in Ref. [36], where the authors of RacoonWW show that, when they include the latter corrections in their predictions for the $\cos\theta_\gamma$ distribution in Fig. 1a, the discrepancy is reduced to the level of $\lesssim 5\%$. In summary, from the results in Ref. [13] and those presented here, we see that the FSR and EW corrections are necessary for a precision study of the distributions in the W-pair production and decay process at LEP2 energies.

We have made a detailed comparison between our results and those from Ref. [16] based on the program RacoonWW in the context of the LEP2 MC Workshop [11]. A complete unpublished preliminary description of the respective results of this comparison has appeared in Ref. [11]. Here, we focus on the normalization comparison of the two calculations at LEP2 energies. We show in Table 3 the comparison of the RacoonWW and YFSWW3-1.14 results for the cross sections as indicated, without cuts at 200 GeV (we have looked at the lower energies 184 and 189 GeV and the comparisons there are similar, if not better). In Table 4, we show the analogous comparisons with the LEP2 MC Workshop cuts as described in Ref. [11].

We see that for all channels considered, the two sets of results agree to the level of 0.3%. This gives a total precision estimate of 0.4% for the theoretical uncertainty on the 200 GeV CMS energy WW signal cross-section normalization when allowance is made for further possible uncertainties in the higher-order radiative corrections and the implementation of the LPA [11]. This is a significant improvement over the originally quoted $\sim 2\%$ for this

uncertainty when the NL non-ISR $\mathcal{O}(\alpha)$ corrections are not taken into account [37]. An effort to further reduce this 0.4% is in progress.

Finally, with an eye toward the LC projects, we have made simulations using YFSWW3-1.14 for a CMS energy of 500 GeV. We show our results in Table 5 for the total cross section without cuts; here we again compare them to the corresponding ones from RacoonWW [16]. The NL corrections are significant in these results. Precision studies at LC energies must take these effects into account. As expected, the percentage difference between YFSWW3-1.14 and RacoonWW remains below 0.5% at 500 GeV CMS energy and is somewhat larger than at 200 GeV CMS energy.

In summary, we have presented two recipes for combining YFSWW3 and KoralW-1.42 to arrive at a gauge-invariant calculation of the WW-pair production and decay in which the YFS-exponentiated exact $\mathcal{O}(\alpha)_{prod}$ corrections are taken into account as well as the $\mathcal{O}(\alpha^2)$ LL FSR and YFS-exponentiated $\mathcal{O}(\alpha^3)$ LL ISR correction to the background processes. We have illustrated our calculation with several sample MC results and we have compared our results on the cross-section normalization with those on Refs. [11] at 200 GeV. In this way, new precision tag of 0.4% has been established for this normalization, which represents a considerable improvement over the original result [37] of $\sim 2\%$ when NL non-ISR corrections are not taken into account.

Acknowledgments

Two of us (S.J. and B.F.L.W.) acknowledge the kind hospitality of Prof. A. De Rújula and the CERN Theory Division while this work was being completed. Three of us (B.F.L.W., W.P. and S.J.) acknowledge the support of Prof. D. Schlatter and of the ALEPH, DELPHI, L3 and OPAL Collaborations in the final stages of this work. S.J. is thankful for the kind support of the DESY Directorate and Z.W. acknowledges the support of the L3 Group of ETH Zurich during the time this work was performed. All of us thank the members of the LEP2 MC Workshop for valuable interactions and stimulation during the course of this work. The authors especially thank Profs. A. Denner, S. Dittmaier and F. Jegerlehner and Drs. M. Roth and D. Wackeroth for useful discussions and interactions.

References

[1] G. 't Hooft and M. Veltman, Nucl. Phys. **B44**,189 (1972) and **B50**, 318 (1972); G. 't Hooft, *ibid.* **B35**, 167 (1971); M. Veltman, *ibid.* **B7**, 637 (1968).

[2] S.L. Glashow, Nucl. Phys. **22** (1961) 579;
S. Weinberg, Phys. Rev. Lett. **19** (1967) 1264;
A. Salam, in *Elementary Particle Theory*, ed. N. Svartholm (Almqvist and Wiksells, Stockholm, 1968), p. 367.

[3] W. Beenakker et al., *WW Cross-Sections and Distributions*, in *Physics at LEP2*, edited by G. Altarelli, T. Sjöstrand and F. Zwirner (CERN 96-01, Geneva, 1996), Vol. 1, p. 79.

[4] W. Beenakker, F. A. Berends and A. P. Chapovsky, Phys. Lett. **B435** (1998) 233; preprint hep-ph/9805327.

[5] W. Beenakker, F. A. Berends and A. P. Chapovsky, preprint hep-ph/9811481; Nucl. Phys. **B548** (1999) 3; preprint hep-ph/9902333.

[6] D. L. Burke, in Beyond the Standard Model 4, eds. J. F. Gunion *et al.* (World Sci. Publ. Co., Singapore, 1995), p. 125.

[7] Y. Kurihara, ed., Japan Linear Collider (JLC) Proceedings,5th Workshop (KEK, Tsukuba, 1995).

[8] M. Piccolo, in Frascati 1998, Bruno Touschek and the Birth of e^+e^- Physics, ed. G. Isidori (INFN, Frascati, 1999), p. 131.

[9] P. M. Zerwas, preprint DESY-99-178, hep-ph/0003221.

[10] S. Jadach *et al.*, to appear.

[11] Proc. of LEP2 MC Workshop, eds., S. Jadach, G. Passarino and F. Pittau, hep-ph/0005309, hep-ph/0007180, Report CERN 2000-009.

[12] S. Jadach, W. Płaczek, M. Skrzypek, B.F.L. Ward and Z. Wąs, Phys. Lett. **B417** (1998) 326.

[13] S. Jadach, W. Płaczek, M. Skrzypek, B.F.L. Ward and Z. Wąs, Phys. Rev. **D61** (2000) 113010, preprint CERN/TH-99-222, hep-ph/9907436.

[14] S. Jadach, W. Płaczek, M. Skrzypek, B. F. L. Ward and Z. Wąs, Comput. Phys. Commun. **119** (1999) 272 and **94** (1996) 216.

[15] M. Skrzypek *et al.*, Phys. Lett. **B372** (1996) 289.

[16] A. Denner, S. Dittmaier, M. Roth and D. Wackeroth, preprints hep-ph/9912261, 9912290, 9912447; Phys. Lett. B**475** (2000) 127; BI-TP 2000/06, hep-ph/0006307; private communication.

[17] R. J. Eden, P. V. Landshoff, D. I. Olive and J. C. Polkinghorne, *The Analytic S-Matrix*, (Cambridge University Press, Cambridge, 1966).

[18] R. G. Stuart, Nucl. Phys. **B498** (1997) 28; Eur. Phys. J. **C4** (1998) 259; hep-ph/9706431, 9706550.

[19] D. R. Yennie, S. Frautschi and H. Suura, Ann. Phys. **13** (1961) 379.

[20] S. Jadach, W. Płaczek, M. Skrzypek and B.F.L. Ward, Phys. Rev. **D54** (1996) 5434.

[21] B.F.L. Ward, Phys. Rev. D**36** (1987) 939; *ibid.* **42** (1990) 3249.

[22] W. Beenakker *et al.*, Nucl. Phys. **B500** (1997) 255.

[23] C. G. Callan, Jr., Phys. Rev. D**2** (1970) 1541; K. Symanzik, Commun. Math. Phys. **18** (1970) 227, and in *Springer Tracts in Modern Physics*, ed. G. Hohler (Springer, Berlin, 1971), Vol. 57, p. 222.

[24] S. Weinberg, Phys. Rev. D **8** (1973) 3497.

[25] See for example W. Beenakker *et al.*, Nucl. Phys. **B500** (1997) 255, and Sect. 3.8 of Ref. [11], references therein.

[26] J. Fleischer, F. Jegerlehner and M. Zrałek, Z. Phys. **C42** (1989) 409;
M. Zrałek and K. Kołodziej, Phys. Rev. **D43** (1991) 43;
J. Fleischer, K. Kołodziej and F. Jegerlehner, Phys. Rev. **D47** (1993) 830;
J. Fleischer *et al.*, Comput. Phys. Commun. **85** (1995) 29 and references therein.

[27] S. Jadach and B.F.L. Ward, Phys. Lett. **B274** (1992) 470.

[28] S. Jadach, B.F.L. Ward and Z. Wąs, CERN-TH/2000-087, hep-ph/0006359.

[29] S. Jadach, B.F.L. Ward and Z. Wąs, Comput. Phys. Commun. **79** (1994) 503.

[30] S. Jadach, W. Płaczek and B.F.L. Ward, Phys. Lett. **B390** (1997) 298.

[31] S. Jadach, B.F.L. Ward and Z. Wąs, Phys. Lett. **B449** (1999) 97; Comput. Phys. Commun. **130** (1999) 260.

[32] E. Barberio and Z. Wąs, Comput. Phys. Commun. **79** (1994) 291 and references therein.

[33] A. P. Chapovsky and V. A. Khoze, hep-ph/9902343; Eur. Phys. J. **C9** (1999) 449.

[34] S. Jadach, W. Płaczek, M. Skrzypek, B.F.L. Ward and Z. Wąs, hep-ph/0103163; hep-ph/0104049.

[35] V.S. Fadin, V.A. Khoze, A.D. Martin and W.J. Stirling, Phys. Lett. **B363** (1995) 112; D. Bardin *et al.*, Phys. Lett. **B317** (1993) 213, and references therein.

[36] A. Denner, S. Dittmaier, M. Roth, and D. Wackeroth, hep-ph/0104057.

[37] D. G. Charlton, hep-ex/9912019, and references therein.

No cuts		σ_{WW} [fb]		δ_{4f} [%]		δ^{NL}_{WW} [%]
Final state	Program	Born	ISR	Born	ISR	
$\nu_\mu\mu^+\tau^-\bar{\nu}_\tau$	YFSWW3	219.793 (16)	204.198 (09)	—	—	−1.92 (4)
	KoralW	219.766 (26)	204.178 (21)	0.041	0.044	—
	(Y−K)/Y	0.01 (1)%	0.01 (1)%	—	—	—
$u\bar{d}\mu^-\bar{\nu}_\mu$	YFSWW3	659.69 (5)	635.81 (3)	—	—	−1.99 (4)
	KoralW	659.59 (8)	635.69 (7)	0.073	0.073	—
	(Y−K)/Y	0.02 (1)%	0.02 (1)%	—	—	—
$u\bar{d}s\bar{c}$	YFSWW3	1978.37 (14)	1978.00 (09)	—	—	−2.06 (4)
	KoralW	1977.89 (25)	1977.64 (21)	0.060	0.061	—
	(Y−K)/Y	0.02 (1)%	0.02 (1)%	—	—	—

Table 1: The total WW cross sections $\sigma_{WW} = \sigma(K_3), \sigma(Y_4)$ at the Born and ISR level, the $4f$ corrections $\delta_{4f} = \Delta\sigma(K)/\sigma_{Born}(Y)$ and the $\mathcal{O}(\alpha)$ NL correction $\delta^{NL}_{WW} = \Delta\sigma(Y_a)/\sigma_{Born}(Y)$ at $E_{CM} = 200$ GeV. The numbers in parentheses are the statistical errors corresponding to the last digits of the results. All of the results are without cuts.

With cuts		σ_{WW} [fb]		δ_{4f} [%]		δ^{NL}_{WW} [%]
Final state	Program	Born	ISR	Born	ISR	
$\nu_\mu\mu^+\tau^-\bar{\nu}_\tau$	YFSWW3	210.938 (16)	196.205 (09)	—	—	−1.93 (4)
	KoralW	210.911 (26)	196.174 (21)	0.041	0.044	—
	(Y−K)/Y	0.01 (1)%	0.02 (1)%	—	—	—
$u\bar{d}\mu^-\bar{\nu}_\mu$	YFSWW3	627.22 (5)	605.18 (3)	—	—	−2.00 (4)
	KoralW	627.13 (8)	605.03 (7)	0.074	0.074	—
	(Y−K)/Y	0.01 (1)%	0.02 (1)%	—	—	—
$u\bar{d}s\bar{c}$	YFSWW3	1863.60 (15)	1865.00 (09)	—	—	−2.06 (4)
	KoralW	1863.07 (25)	1864.62 (21)	0.065	0.064	—
	(Y−K)/Y	0.03 (2)%	0.02 (1)%	—	—	—

Table 2: The total WW cross sections $\sigma_{WW} = \sigma(K_3), \sigma(Y_4)$ at the Born and ISR level, the $4f$ corrections $\delta_{4f} = \Delta\sigma(K)/\sigma_{Born}(Y)$ and $\mathcal{O}(\alpha)$ NL correction $\delta^{NL}_{WW} = \Delta\sigma(Y_a)/\sigma_{Born}(Y)$ at $E_{CM} = 200$ GeV. The numbers in parentheses are the statistical errors corresponding to the last digits of the results. All of the results are with the *bare* cuts of Sect. 4.1 of Ref. [11].

No cuts		$\sigma_{\rm tot}$[fb]	
final state	program	Born	best
$\nu_\mu\mu^+\tau^-\bar{\nu}_\tau$	YFSWW3	219.770(23)	199.995(62)
	RacoonWW	219.836(40)	199.551(46)
	(Y–R)/Y	−0.03(2)%	0.22(4)%
$u\bar{d}\mu^-\bar{\nu}_\mu$	YFSWW3	659.64(07)	622.71(19)
	RacoonWW	659.51(12)	621.06(14)
	(Y–R)/Y	0.02(2)%	0.27(4)%
$u\bar{d}s\bar{c}$	YFSWW3	1978.18(21)	1937.40(61)
	RacoonWW	1978.53(36)	1932.20(44)
	(Y–R)/Y	−0.02(2)%	0.27(4)%

Table 3: Total cross-sections for CC03 from RacoonWW and YFSWW3 at $\sqrt{s} = 200\,\text{GeV}$ without cuts. The numbers in parentheses are statistical errors corresponding to the last digits.

With *bare* cuts		$\sigma_{\rm tot}$[fb]	
final state	program	Born	best
$\nu_\mu\mu^+\tau^-\bar{\nu}_\tau$	YFSWW3	210.918(23)	192.147(63)
	RacoonWW	211.034(39)	191.686(46)
	(Y–R)/Y	−0.05(2)%	0.24(4)%
$u\bar{d}\mu^-\bar{\nu}_\mu$	YFSWW3	627.18(07)	592.68(19)
	RacoonWW	627.22(12)	590.94(14)
	(Y–R)/Y	−0.01(2)%	0.29(4)%
$u\bar{d}s\bar{c}$	YFSWW3	1863.40(21)	1826.80(62)
	RacoonWW	1864.28(35)	1821.16(43)
	(Y–R)/Y	−0.05(2)%	0.31(4)%

Table 4: Total cross-sections for CC03 from YFSWW3 and RacoonWW at $\sqrt{s} = 200\,\text{GeV}$ with *bare* cuts of Sect. 4.1 in Ref. [11] (see the text). The numbers in parentheses are statistical errors corresponding to the last digits.

No cuts		$\sigma_{\rm tot}$[fb]	
Final state	Program	Born	Best
$\nu_\mu\mu^+\tau^-\bar{\nu}_\tau$	YFSWW3	87.087(11)	89.607(32)
	RacoonWW	87.133(23)	90.018(27)
	(Y–R)/Y	−0.05(3)%	−0.46(5)%
$u\bar{d}\mu^-\bar{\nu}_\mu$	YFSWW3	261.377(34)	279.086(97)
	RacoonWW	261.400(70)	280.149(86)
	(Y–R)/Y	−0.01(3)%	−0.38(5)%
$u\bar{d}s\bar{c}$	YFSWW3	783.93(11)	868.14(31)
	RacoonWW	784.20(21)	871.66(27)
	(Y–R)/Y	−0.03(3)%	−0.41(5)%

Table 5: Total cross-sections for CC03 from RacoonWW and YFSWW3 at $\sqrt{s} = 500\,\text{GeV}$ without cuts. The numbers in parentheses are statistical errors corresponding to the last digits.

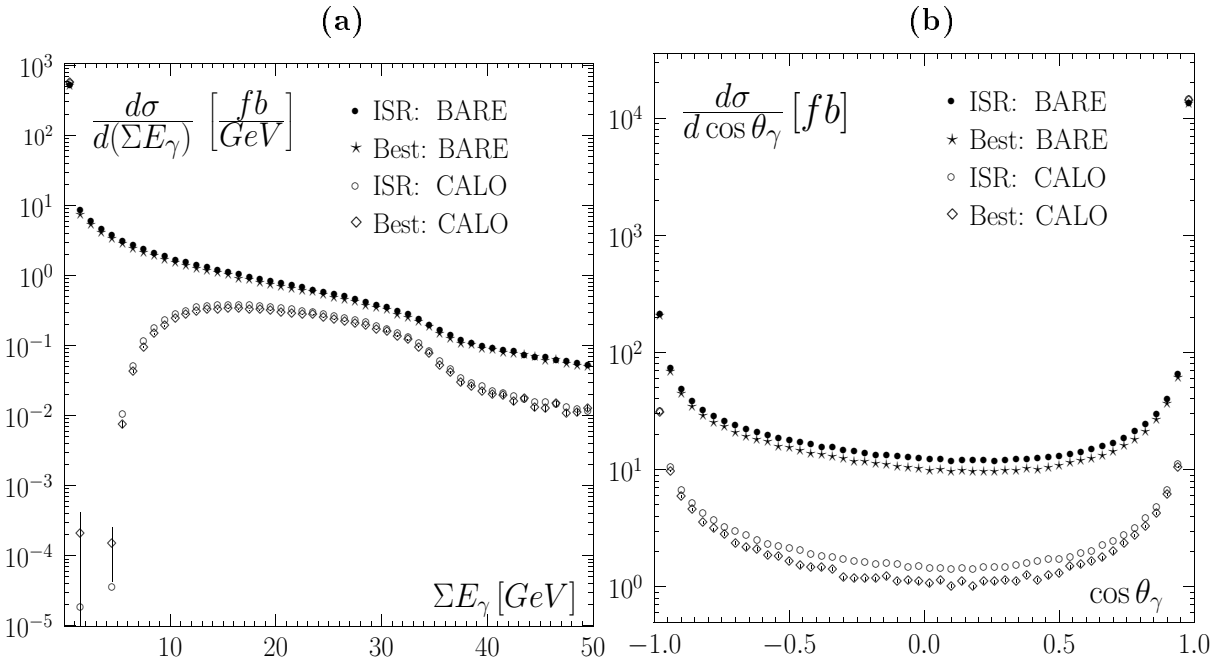

Figure 1: Distributions of the total photon energy (a) and cosine of the hardest photon polar angle (b) for the $u\bar{d} + \mu\bar{\nu}_\mu + n(\gamma)$ final-state. The solid, open circle, star, and diamond curves correspond to the LL BARE, LL CALO, $\mathcal{O}(\alpha)_{prod}$ $\mathcal{O}(\alpha^2)$ LL FSR BARE and CALO YFS-exponentiated results, respectively.

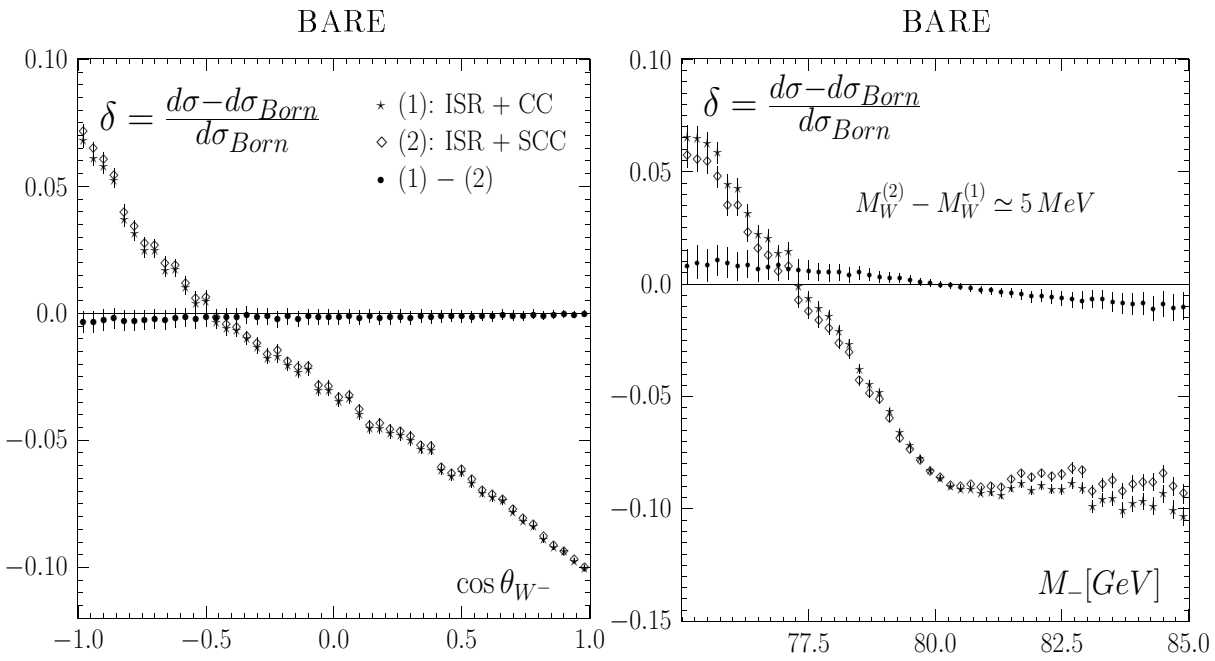

Figure 2: Effects of the screened Coulomb correction (SCC) on the distributions of the polar angle (left) and the invariant mass (right) of W^- in comparison with the usual Coulomb correction (CC) at $E_{CM} = 200\,\text{GeV}$. As indicated the star, solid diamond and large dot curves are the ISR + usual Coulomb correction, ISR + screened Coulomb correction and their difference respectively, in the presence of YFS-exponentiation. Results are for the $e^+e^- \longrightarrow W^+W^- \longrightarrow u\bar{d}\mu^-\bar{\nu}_\mu$ channel. The *bare* cut is that of Sect. 4.1 of Ref. [11].